Available online at www.sciencedirect.com
SCIENCE DIRECT
Thermochimica Acta 447 (2006) 161–166
thermochimica acta
www.elsevier.com/locate/tca

Kinetics study of the SO_2 sorption by Brazilian dolomite using thermogravimetry

P.M. Crnkovic *, F.E. Milioli, J.D. Pagliuso

School of Engineering of São Carlos, University of São Paulo, São Carlos 13560-970, Brazil

Received 23 March 2006; received in revised form 25 May 2006; accepted 26 May 2006
Available online 3 June 2006

Abstract

Sulfur emission in coal power generation is a matter of great environmental concern. Limestone sorbents are widely used for reducing such emissions. This work applies thermogravimetry to determine apparent activation energy and frequency factor on the sorption of SO_2 by limestone. The kinetic parameters were determined from Arrhenius plots generated from TG/DTG measurements. The experiments were carried out under isothermal conditions between 600 and 900 °C. A natural dolomite with a mean size of 650 μm was used. The Arrhenius plot shows that there is a clear change on reaction mechanism in the range of temperatures between 800 and 875 °C. Supposedly, beyond 850 °C sintering comes to increasingly restrain reaction. For temperatures up to 850 °C the frequency factor and the apparent activation energy resulted, respectively, 1.410 s^{-1} and 8.8 kJ mol^{-1}.

Keywords: Sulfation; Kinetics; Thermogravimetry; Dolomite

1. Introduction

Fluidized bed desulfurization by limestone sorbents is an efficient technology for sulfur removal in the combustion of fuels of high sulfur content. The fluid bed process is suitable for burning any material containing carbon and hydrogen, no matter it is gaseous, solid, liquid, slurry, sludge, etc. Concerning large-scale utilization, besides the obvious coal combustion, fluidized beds have been considered for burning a range of high sulfur petrol derivatives (e.g. heavy oils, tars, coke, residues, etc.) [1].

Desulfurization under combustion is a quite complex process. Besides chemical kinetics, the rates of reaction are considerably affected by transport both intra-particle and throughout the combustion environment. This work aims to contribute to the discussion regarding the determination of reaction rates controlled by the combined effects of kinetics and intra-particle transport. As composed to ambience transport conditions, the intrinsic rates allow to establish the actual rate of reaction in a complex process such as fluidized bed combustion.

The calcium oxide is frequently considered a sorbent to desulfurization in the burning process. When a natural limestone is injected into the high temperature ambience of a fluidized bed combustor, it is thermally decomposed and calcination takes place, i.e.

$$CaCO_3 + MgCO_3 \rightarrow CaO + MgO + 2CO_2 \quad (1)$$

After calcination CaO reacts with SO_2 and O_2 to form $CaSO_4$ accomplishing the sulfation step. MgO may also sulfate to form $MgSO_4$ at moderate temperatures [2]. The global sulfation may be given by

$$CaO + MgO + 2SO_2 + O_2 \rightarrow CaSO_4 + MgSO_4 \quad (2)$$

The actual mechanism leading to the formation of $CaSO_4$ is still a subject of controversy among researchers. However, it is generally accepted that the reaction between the porous solid CaO and the gas SO_2 (in oxidizing atmosphere) is first order related to SO_2. It is also generally agreed that sulfation rate is maximum at temperatures around 850 °C [3].

The capability of sorption of a sorbent is ultimately determined by its porous structure, that allows reactive gases to access internal active sites and make room for accumulating the product sulfate. The sulfation reaction goes fast in the first

* Corresponding author. Tel.: +55 16 33739557; fax: +55 16 33739402.
E-mail address: paulam@sc.usp.br (P.M. Crnkovic).

0040-6031/$ – see front matter © 2006 Elsevier B.V. All rights reserved.
doi:10.1016/j.tca.2006.05.023

few seconds. Then, it becomes limited by growing resistances to gas diffusion, either external or intra-particle, or a combination of both [4]. Pore plugging accounts for growing intra-particle gas diffusion resistances. The blockage of pores is favored by the fact that the molar volume of $CaSO_4$ is 172% higher than that of CaO, and the formed product layer is essentially non-porous [5]. As the thickness of the product layer increases, gas diffusion becomes slower and the reaction rate decreases exponentially [6]. Of course, the higher the temperature the faster the kinetics, and the higher the sulfation rate. However, at temperatures sufficiently high the rate of reaction turns to decrease. Such is commonly attributed to either sintering or re-emission of SO_2 due to a possible decomposition of sulfates [7]. The last effect is relevant in combustion reductive atmospheres [8].

Many authors have studied sulfation in thermogravimetric analysis systems. Some of them apply atmospheres with fractions of CO_2 high enough to inhibit $CaCO_3$ calcination. Sulfation under such conditions has been referred to as direct sulfation ($CaCO_3$–SO_2) [5,9–12]. In some cases, high concentrations of CO_2 are used to simulate the ambience of a fluidized bed combustor. In those conditions direct sulfation of $CaCO_3$ is showed to proceed to high conversion, in contrast to the relatively lower sulfation extent of previously calcined limestones. Snow et al. [5] reported thermogravimetric non-isothermal studies of $CaCO_3$ sulfation for six different particle sizes, in 95% CO_2 atmosphere. The authors found an apparent activation energy of 64.1 kJ mol^{-1}. Hajaligol et al. [6] developed experiments similar to those of Snow et al. [5] but under isothermal conditions. Notwithstanding, they found results in accordance to those of Snow and co-workers. The authors came to the expected conclusion that diffusivities depend on porosity. Their research showed that under direct sulfation the product sulfate layers become more porous owing to the simultaneous generation of CO_2. The passage of CO_2 through the sulfate layers leads to a more open structure, thereby allowing an easier access of SO_2 and O_2 to under layer CaO active sites. As a consequence, direct sulfation turned out to be more effective that the sulfation of previously calcined limestone.

Van Houte and Delmon [11] investigated the $CaCO_3$–SO_2 reaction at low temperatures to avoid calcination. At around 550 °C and low conversions, the authors found an apparent activation energy of 210 kJ mol^{-1}. For 60% conversion they found 110 kJ mol^{-1}. Li and Sadakata [13] determined the apparent activation energy for sulfation with both CaO and $CaO{\cdot}Al_2O_3$, thereby evaluating the effect of Al_2O_3 on SO_2 removal. They found apparent activation energies of 7.29 kJ mol^{-1} for pure CaO, and 9.21 kJ mol^{-1} for $CaO{\cdot}Al_2O_3$, and concluded that $CaO{\cdot}Al_2O_3$ is more active on the dessulfurization.

All the concerning sulfation literature presents apparent activation energies which are time averaged, since the physical structure of limestones and thereby chemical kinetics change on time. Reaction mechanisms change from kinetic control at lower temperatures to diffusion control at higher temperatures, which is intensified as pore plugging advances. It becomes quite clear that the apparent activation energy considerably changes during conversion.

In this work isothermal thermogravimetry is applied to determine apparent activation energy and frequency factor on the sorption of SO_2 by a particular dolomite, considering Arrhenius kinetic.

1.1. Basic theory and method

Following the global sulfation reaction in Eq. (2), reaction rate results

$$\frac{\mathrm{d}m}{\mathrm{d}t} \propto -mC_{\mathrm{SO_2}}^{a}C_{\mathrm{O_2}}^{b} \tag{3}$$

where m stands for the mass of Ca plus Mg available for sulfation; C_{SO_2} and C_{O_2} are the concentrations of the reactive gases in the atmosphere; a and b are reaction orders related to each reactant gas. The reaction is assumed first order related to the sample mass. Differential conditions [4,14,15] are imposed by applying high concentrations of the reactant gases in the atmosphere (20%), so that transport effects external to the particles are eliminated and the reaction results controlled by intrinsic or intra-particle kinetics and diffusion mechanisms. As a consequence, the reaction becomes independent of gas concentrations, i.e., pseudo zeroth order related to both SO_2 and O_2 ($a = b = 0$). The ultimate rate of reaction results

$$\frac{\mathrm{d}m}{\mathrm{d}t} \propto -m \tag{4}$$

Introducing a reaction rate coefficient (k), it comes that

$$\frac{\mathrm{d}m}{\mathrm{d}t} = -km \tag{5}$$

Arrhenius kinetics is followed to account for reaction rate dependence on temperature, i.e.

$$k = A\exp\left(-\frac{E_{\mathrm{a}}}{RT}\right) \tag{6}$$

Then, Eq. (5) becomes

$$-\frac{1}{m}\frac{\mathrm{d}m}{\mathrm{d}t} = A\exp\left(-\frac{E_{\mathrm{a}}}{RT}\right) \tag{7}$$

or

$$\ln\left[-\frac{1}{m}\frac{\mathrm{d}m}{\mathrm{d}t}\right] = \ln[A] - \frac{E_{\mathrm{a}}}{R}\frac{1}{T} \tag{8}$$

From empirical data of m, $\mathrm{d}m/\mathrm{d}t$ and process temperature, and applying Eq. (8), an Arrhenius' plot can be constructed, which allows to derive A and E_{a} by linear regression. The mass of Ca plus Mg available for sulfation and its time rate can be determined from a mass balance. Assuming Ca and Mg to be sulfated at the some rate, it comes that:

$$m = M_{\mathrm{L}}(Y_{\mathrm{Ca}} + Y_{\mathrm{Mg}}) - \left(\frac{m_{\mathrm{s}} - m_{\mathrm{c}}}{W_{\mathrm{SO_2}} + 0.5W_{\mathrm{O_2}}}\right) \times \left(\frac{Y_{\mathrm{Ca}}W_{\mathrm{Ca}} + Y_{\mathrm{Mg}}W_{\mathrm{Mg}}}{Y_{\mathrm{Ca}} + Y_{\mathrm{Mg}}}\right) \tag{9}$$

and

$$\frac{dm}{dt} = -\left(\frac{Y_{Ca}W_{Ca} + Y_{Mg}W_{Mg}}{(W_{SO_2} + 0.5W_{O_2})(Y_{Ca} + Y_{Mg})}\right)\frac{dm_s}{dt} \quad (10)$$

where m_s is the mass of sulfated material at a given reaction stage (TG result) and dm_s/dt stands for its time rate (DTG result); m_c is the mass of calcined limestone (i.e. the mass of the sample before sulfation); M_L is the initial mass of the sample (i.e. the mass of the sample before calcination); Y accounts for the mass fraction of the concerning species in the natural limestone; and W is the molecular mass of the concerning species.

The reaction rate on limestone sulfation is inherently variable since the physical structure of the rock changes during the process. The reaction experiments an enhancement in its early stages while the reactive gases flow into the reactive solid particles. Then, intra-particle diffusion resistances become progressively intensified notably owing to pore plugging, causing the reaction rate to progressively decay. There is a stage along the process on which a maximum reaction rate is found. Such is identified by a pick on a DTG curve. In this work the kinetic parameters are determined for this stage of maximum reaction rate.

At the maximum reaction rate spot, the reaction rate coefficient is given by

$$k_{max} = \left[-\frac{1}{m}\frac{dm}{dt}\right]_{max} \quad (11)$$

or

$$k_{max} = \left[-\frac{((Y_{Ca}W_{Ca} + Y_{Mg}W_{Mg})/((W_{SO_2} + 0.5W_{O_2})(Y_{Ca} + Y_{Mg})))(dm_s/dt)}{M_L(Y_{Ca} + Y_{Mg}) - ((m_s - m_c)/(W_{SO_2} + 0.5W_{O_2})((Y_{Ca}W_{Ca} + Y_{Mg}W_{Mg})/Y_{Ca} + Y_{Mg}))}\right]_{max} \quad (12)$$

2. Experimental

The thermogravimetric analysis was carried out in a Shimadzu 51H unit with a high-temperature furnace (up to 1500 °C). The procedure consisted of heating a sorbent sample at 30 °C min^{-1} until a desired temperature was reached. Synthetic air was continuously blown through the furnace over the sample at a volumetric rate of 80 mL min^{-1} as a carrier gas. When an isothermal condition was reached, 20 mL min^{-1} of pure SO_2 (100% v/v) was added to ensure a volumetric fraction of the gas in the furnace atmosphere of 20%. Under these conditions, the reaction rate was found based on the shape of TG and DTG curves (correct for buoyancy).

Isothermal TG sulfation experiments were performed at 600, 650, 700, 750, 800, 850, 875 and 900 °C. In the experiments at 600, 650, 700 and 750 °C, the temperature was firstly raised to 850 °C under synthetic air atmosphere in order to guarantee a complete calcination. Then, the temperature was reduced at a rate of 30 °C min^{-1} until a temperature desired for sulfation was reached. Five replicate experiments were carried out on each temperature.

A Brazilian dolomite from São Paulo State was used in this study. The rock was grinded and sieved to an average particle size of 650 μm. The average size of the particles was determined as the arithmetic mean between the mesh apertures of two consecutive ASTM laboratory sieves. The particular 650 μm particle size was chosen so that decrepitation effects were avoided [16], and considering it is a size common to fluidized bed combustion applications. Chemical analysis and RXD of the natural dolomite are shown in Table 1 and Fig. 1, respectively.

Table 1
Partial chemical analysis of the dolomite (wt.%)

Element	wt.%
Sr	0.0811
Mn	0.0888
Ba	0.0054
K	0.097
P	0.0554
Fe	0.3207
Al	0.4233
Ca	17.07
Mg	11.72

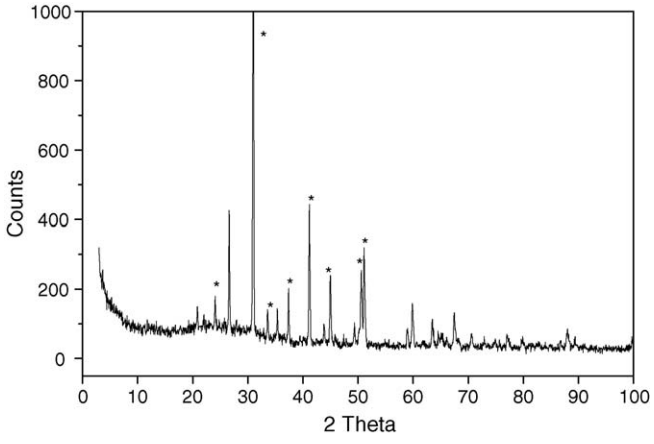

Fig. 1. X-ray diffraction of the natural Brazilian dolomite. ⋆: $CaMg(CO_3)_2$.

Samples weighing 10.0 ± 0.5 mg were used throughout the experiments. This mass of dolomite allows minimizing interparticle mass transfer resistances by spreading the particles in a monolayer on the bottom of the crucible (alumina, Ø 6 mm × 2.5 mm).

The reaction solid products were analyzed through X-ray diffraction in a 2θ range of 20–70°. A supplementary study was performed to clarify the reactivity to SO_2 of both CaO and MgO. In such study reagent-grade samples of $CaCO_3$ and $MgCO_3$ were submitted to calcination followed by isothermal sulfation at 850 °C in TG experiments.

3. Results and discussion

Fig. 2 shows TG and DTG curves for one of the performed experiments of calcination followed by sulfation. In this case, the isothermal condition was established at 850 °C. The data

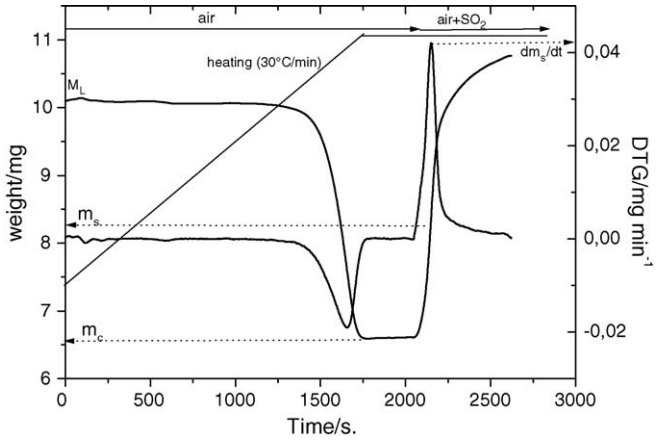

Fig. 2. TG and DTG curves for one of the performed experiments of calcination followed by sulfation. The temperature of the isothermal step is 850 °C.

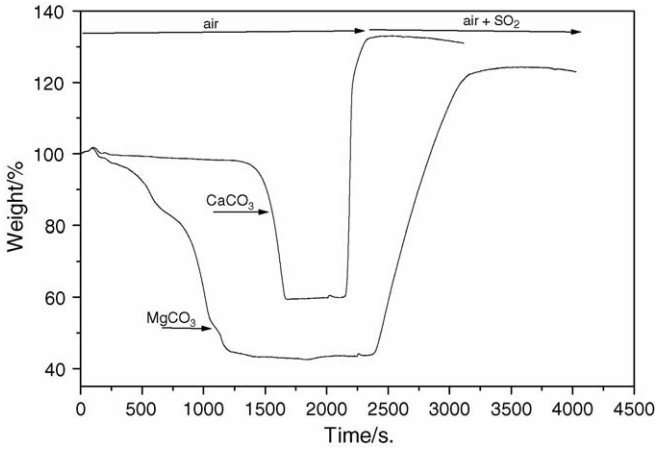

Fig. 4. TG curves of calcination followed by sulfation for reagent-grade samples of $CaCO_3$ and $MgCO_3$.

show that sulfation presents two consecutive different behaviors. At first it advances very quickly turning to advance slowly afterwards. In the first step the reaction is very fast owing to kinetics control. The second step is slower owing to a growing diffusion resistance to reaction imposed by pore plugging. As it can be observed the mass gain in sulfation is not proportional to the mass loss during the calcination.

The XRD spectrum of sulfated dolomite is shown in Fig. 3. According to the JCPDS file the main peak for $CaSO_4$ appears at $2\theta = 25.5°$, and the minor peaks appear at $2\theta = 30.3°$, 36.0°, 39.6° and 51.1°. For $MgSO_4$ the main peaks appear at $2\theta = 24.9°$ and 25.1, and the minor peak, at $2\theta = 21.4°$.

Even though $CaSO_4$ and possibly $MgSO_4$ have been detected, it is quite difficulty to distinguish the main peaks of $CaSO_4$ and $MgSO_4$ in the XRD spectrum. So, in order to prove the sulfation reaction of both CaO and MgO, investigations were made through thermogravimetry. TG curves of calcination followed by sulfation obtained with reagent-grade samples ($CaCO_3$ and $MgCO_3$) are shown in Fig. 4. As it can be seen, the gain of mass was obtained for both sorbents. From this observation, it was assumed that the MgO reacts with SO_2.

Table 2 gives M_L, m_s, m_c, dm_s/dt, and $\ln[(-1/m)(dm/dt)]_{max}$ averaged over five replicated experiments for each process temperature. Fig. 5 shows an Arrhenius plot giving the dispersion around the average values reported in Table 2.

The relatively high dispersions are possibly due to the heterogeneity of the sample, since it deals with natural limestone extracted directly from mine and size distribution. It can be seen from Table 2 and Fig. 5 that reaction rate increases with increasing temperatures up to 850 °C, owing to increasingly faster kinetics. The reaction rate drops for temperatures above 875 °C. As seen, there is a clear change on reaction mechanism in the range of temperatures between 800 and 875 °C. Supposedly, beyond 850 °C sintering comes to increasingly restrain reaction. Such decrease seems to be a consequence of sintering (SO_2 re-emission is discarded since no combustion reductive atmosphere is applied).

An Arrhenius plot for sulfation up to 850 °C is showed in Fig. 6. For the whole range of temperatures, up to 850 °C, a linear regression provides a frequency factor of 1.410 s^{-1} and an apparent activation energy of 8.8 kJ mol^{-1}. In the range from 600 to 700 °C the frequency factor and the apparent activation

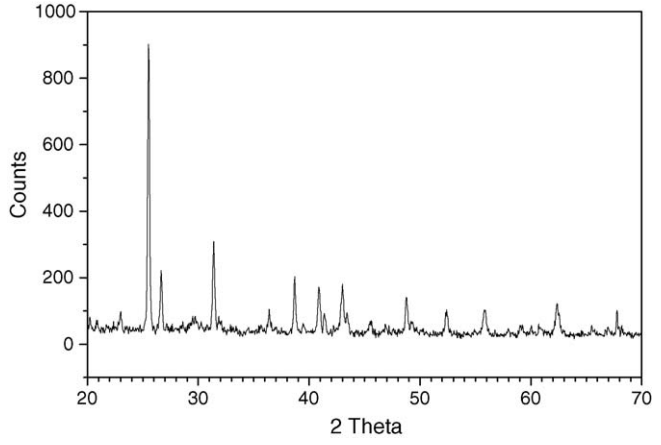

Fig. 3. X-ray diffraction pattern of the products $CaSO_4$ ($2\theta = 25.5°$, 30.3°, 36.0°, 39.6° and 51.1°) and $MgSO_4$ ($2\theta = 24.9°$, 25.1°, 21.4°).

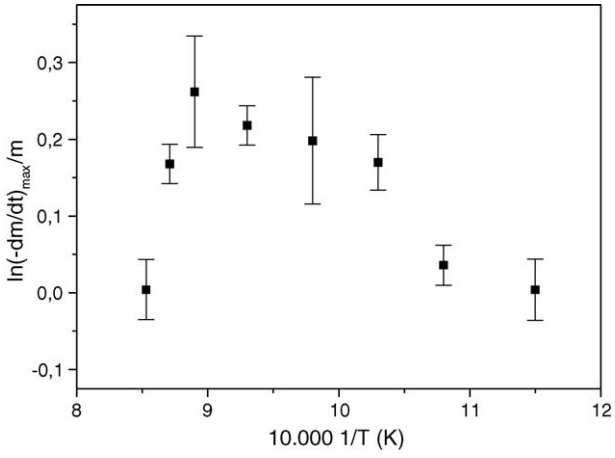

Fig. 5. Arrhenius plot showing the dispersion around the averaged values of $\ln[(-1/m)(dm/dt)]_{max}$ reported in Table 2. The bars point the maximum and the minimum values that were found.

Table 2
Values of M_L, m_s, m_c, and dm_s/dt for each process temperature, and $\ln[(-1/m)(dm/dt)]_{max}$ averaged over five replicated experiments

Temperature (°C)	M_L (mg)	m_s (mg)	m_c (mg)	dm_s/dt (mg min^{-1})	Averaged $\ln[(-1/m)(dm/dt)]_{max}$	Tempature 10000/T (K^{-1})
	10.17	7.88	6.58	2.73		
	10.27	7.91	6.54	2.67		
600	9.79	7.67	6.19	2.76	0.01	11.5
	10.02	7.70	6.20	2.55		
	10.32	7.89	6.54	2.70		
	10.31	8.38	6.57	2.66		
	10.08	8.00	6.63	2.84		
650	9.87	8.12	6.50	2.65	0.03	10.8
	9.80	8.1	6.54	2.70		
	10.19	8.67	6.78	2.70		
	9.88	8.25	6.78	3.20		
	10.02	8.19	6.57	3.13		
700	9.71	7.86	6.60	2.98	0.17	10.3
	9.92	7.90	6.30	3.07		
	10.32	8.16	6.35	3.03		
	10.43	8.69	6.84	3.16		
	10.58	8.64	6.96	3.12		
750	10.19	8.31	6.85	3.09	0.20	9.8
	10.29	8.33	6.46	3.62		
	9.76	7.99	6.15	3.27		
	9.83	7.77	6.46	3.35		
	10.05	8.50	6.90	3.30		
800	10.25	8.66	6.99	3.29	0.22	9.3
	10.04	8.45	6.55	3.10		
	10.25	8.75	6.97	3.30		
	9.20	7.27	5.97	3.11		
	9.50	7.04	6.27	3.68		
850	9.74	7.39	6.33	3.55	0.26	8.9
	10.07	8.25	6.58	3.18		
	10.47	8.74	6.79	3.29		
	10.37	8.56	7.01	3.19		
	10.05	8.26	6.57	3.20		
875	10.34	9.03	7.44	3.10	0.17	8.71
	10.09	8.42	6.57	3.16		
	10.04	8.23	6.78	3.08		
	10.54	9.1	7.36	2.85		
	10.18	8.07	6.34	2.50		
900	10.19	8.53	7.12	2.69	0.00	8.53
	10.21	8.41	7.20	2.75		
	9.87	7.98	6.8	2.70		

energy resulted, respectively, 2.037 s^{-1} and 11.6 kJ mol^{-1}. In the range from 700 to 850 °C the parameters resulted, respectively, 0.957 s^{-1} and 5.3 kJ mol^{-1}. This variation on the concerning parameters suggests that at different temperatures the maximum reaction rate finds the particles under different physical structures, and consequently at different balances between kinetic and diffusion control. It should be noted that the present experiments detected only combined effects of kinetics plus intra-particle diffusion, so that the balance between these effects could not be evaluated separately.

Any comparison among results from different works must take into account differences on experimental conditions. One of such conditions refers to the reaction atmosphere. In this work reaction took place in absence of CO_2, and the fractions of SO_2 and O_2 were both 20%. Some literature reported figures on apparent activation energy [5,9–12] considerably differ from those derived in the present work (e.g. 64.1 kJ mol^{-1} [5]). However, the values presented in those reports refer to sulfation in atmosphere with O_2 concentration of 5%, CO_2 concentration ranged from 2 to 95% and SO_2 varying from 600 to 3000 ppm. The low concentrations of SO_2 suggest that differential conditions are not met, and mass transport external to the particles act as an additional resistance to reaction. In addition, the presence of CO_2 in the atmosphere can also affect conversion since it can affect the structure of the product layer.

On the other hand, the apparent activation energies presented here are in good agreement with those presented in Li and Sadakata [13] (7.29 kJ mol^{-1}). Those authors performed experiments in a thermogravimetric balance in absence of CO_2, applying a SO_2 concentration of 3000 ppm. They used a very fine

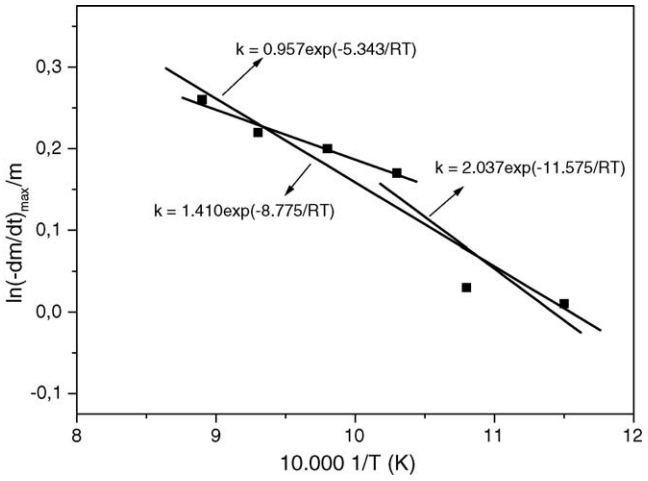

Fig. 6. Arrhenius plot for the sulfation reaction, for temperatures up to 850 °C.

CaO particulate (<45 μm) to reduce pore diffusion effects, and dispersed the particles in quartz wool to minimize inter-particle diffusion effects.

4. Conclusions

The TG/DTG experiments on sulfur sorption by dolomite showed a change on sulfation mechanism at 850 °C. Such was attributed to sintering. SO_2 re-emission was rejected since no combustion reductive atmosphere was applied.

In this work differential conditions were applied so that the concentration of the reactant gases did not affect reaction rates. The relatively high dispersions around the average values over five replicated experiments are possibly due to the heterogeneity of the sample, since it deals with natural limestone extracted directly from mine.

Significant differences were found as the present activation energies were compared to literature available data. It is suggested that maybe those data were not obtained under differential conditions. Besides, it is recognized that the presence of CO_2 in the atmosphere can possibly affect conversion, contributing for the observed differences.

Acknowledgements

This work is part of the research program on mineral coal combustion of NETeF (Thermal and Fluids Engineering Group—University of São Paulo). The program is supported by FAPESP (São Paulo State Research Foundation) and CNPq (Brazilian Council for Scientific and Technological Development) through both scholarships and research grants. The first author is grateful to FAPESP for the doctoral and post-doctoral scholarships (processes 98/14393-3; 04/06894-4).

References

[1] F.M. Okasha, S.H. Hemam, H.K. Mostafa, Exp. Therm. Fluid Sci. 27 (2003) 473–480.
[2] S.S. Tambe, S.S. Yerrapragada, K.L. Guari, J. Mater. Civil Eng. 6 (1994) 65–77.
[3] D. Allen, A. Hayhurst, J. Chem. Soc., Faraday Trans I. 92 (1996) 1227–1228.
[4] M. Hartman, R.W. Coughlin, AIChE J. 22 (1976) 490–498.
[5] M.J.H. Snow, J.P. Longwell, A.F. Sarofim, Ind. Eng. Chem. Res. 27 (1988) 268–273.
[6] A. Lyngfelt, B. Leckner, Chem Eng. Sci 44 (1989) 207–213.
[7] T. Mattisson, A. Lyngfelt, Energy Fuels 12 (1998) 905–912.
[8] K. Lisa, M. Hupa, J. Inst. Energy 65 (1992) 201–205.
[9] M.R. Hajaligol, J.P. Longwell, A.F. Sarofim, Ind. Eng. Chem. Res. 27 (1988) 2203–2210.
[10] A.B. Fuertes, G. Velasco, M.J. Fernandez, T. Alvarez, Thermochim. Acta 242 (1994) 161–172.
[11] G. Van Houte, B. Delmon, J. Chem. Soc., Faraday Trans. I 75 (1979) 1593–1605.
[12] Z. Qin, J. Therm. Anal. 45 (45) (1995) 211–219.
[13] Y. Li, M. Sadakata, Fuel 78 (1999) 1089–1095.
[14] P. Daniell, Soltani-Ahmadi, H.O. Kono, Powder Technol. 55 (1988) 75–85.
[15] S.A. Carello, A.C.F. Vilela, Ind. Eng. Chem. Res. 32 (1993) 3135–3142.
[16] P.M. Crnkovic, W.L. Polito, C.G. Silva Filho, F.E. Milioli, J.D. Pagliuso, Quim. Nova 27 (2004) 58–61.